Eur. Phys. J. A **17**, 25–28 (2003)
DOI 10.1140/epja/i2002-10142-5

THE EUROPEAN PHYSICAL JOURNAL A

# Band termination in the Z = N odd-odd nuclei $^{46}$V and $^{50}$Mn

BaoGuo Dong[a] and HongChao Guo

Department of Nuclear Physics, China Institute of Atomic Energy, P.O. Box 275, Beijing 102413, PRC

Received: 2 April 2002 / Revised version: 18 November 2002 /
Published online: 15 April 2003 – 
Communicated by D. Schwalm

**Abstract.** The configuration-dependent cranked Nilsson-Strutinsky approach has been employed to study the properties and band structures at high spin in the $Z = N$ odd-odd nuclei $^{46}$V and $^{50}$Mn. The observed bands are explained and terminating states are confirmed by the calculations. The calculated and observed bands are in good agreement without normalization, especially for terminating states. Possible bands with rotation around the intermediate axis and the effect of $\gamma$-deformation on the total energy of several interesting configurations are discussed.

**PACS.** 21.10.Hw Spin, parity, and isobaric spin – 21.10.Re Collective levels – 21.60.Ev Collective models – 27.40.+z $39 \leq A \leq 58$

The features of band structures at high spin and smooth band terminations for the $Z = N$ deformed odd-odd nuclei at or near the proton drip line in the $A \sim 40$ mass region are of special interest. The valence space outside the $^{40}$Ca core is large enough for $^{50}$Mn or $^{46}$V to form plenty of interesting band structures. The experimental results of the odd-odd nucleus $^{46}$V [1] was recently reported and the rotational bands were observed up to spin $15^+$, $16^-$ and $17^-$, respectively. Experimentally, the structure of $^{46}$V was studied from different points of view, see refs. [2,3]. One high-spin band was observed in $^{50}$Mn [4,5]. Shell model calculations have been performed [1–5] for $^{46}$V and $^{50}$Mn.

The configuration-dependent cranked Nilsson-Strutinsky (CNS) approach [6,7] has been employed to study the band structures of $^{46}$V and $^{50}$Mn. The Nilsson parameters of ref. [8] have been adopted and pairing correlations have been neglected. Considerable effort has recently focused on even-even or odd-$A$ nuclei, such as $^{48}$Cr [9] and $^{36}$Ar [10], to compare the description of experimental data by the CNS, shell model and cranked Hartree-Fock-Bogoliubov calculations. The CNS calculations are thus expected to provide a reliable description of quadruple properties [9]. For convenience, the shorthand notation used later to label the configurations (relatively to the $^{40}$Ca core) is defined as $[p_1p_2, n_1n_2] \equiv \pi(d_{3/2}s_{1/2})^{-p_1}(f_{7/2})^{p_2} \otimes \nu(d_{3/2}s_{1/2})^{-n_1}(f_{7/2})^{n_2}$. $p_1(n_1)$ and $p_2(n_2)$ are the number of proton (neutron) holes in the $(d_{3/2}s_{1/2})$ orbitals and protons (neutrons) in the $f_{7/2}$ orbitals. $(d_{3/2}s_{1/2})^{-p_1(n_1)}$ will be omitted if $p_1(n_1)$ is zero. In addition, + and − for this shorthand notation will be used in some cases in order to indicate the positive and negative signature orbital occupied by the last proton and neutron.

For $^{46}$V, there are three valence protons and neutrons outside the $^{40}$Ca core which occupy the lowest two orbitals of the $1f_{7/2}$ subshell below the Fermi surface and form ground states or yrast bands when the deformation $\varepsilon_2$ is less than 0.3 according to the single-particle energies diagram. Configurations of excited bands are obtained by exciting one nucleon from the $(d_{3/2}s_{1/2})$ to $f_{7/2}$ orbitals. Configurations of higher excited bands can be formed by making particle-hole excitations and will not be discussed further here because they are unfavored in energy.

In order to understand the observed bands in $^{46}$V and $^{50}$Mn, the CNS calculations have been performed for the four combinations of parity ($\pi = \pm$) and signature ($\alpha = 0, 1$). For $(\pi, \alpha) = (+, 0), (+, 1)$, the configurations of interest near yrast bands and the possible maximum spins obtained for these configurations are [03,03], *i.e.* $\pi[(f_{7/2})^{3\pm}_{6.5,7.5}]_{6.5,7.5} \otimes \nu[(f_{7/2})^{3\pm}_{6.5,7.5}]_{6.5,7.5}$, and $I_{\max} = 13, 14$ and 15, and [14,14], $\pi[(d_{3/2}s_{1/2})^{-1\pm}_{0.5,1.5}(f_{7/2})^4_8]_{8.5,9.5} \otimes \nu[(d_{3/2}s_{1/2})^{-1\pm}_{0.5,1.5}(f_{7/2})^4_8]_{8.5,9.5}$, and $I_{\max} = 17, 18$ and 19, respectively. The plus or minus, $\pm$, in the superscripts indicates the signature $\alpha = -1/2$ or $+1/2$ orbital occupied by the last proton or neutron in that subshell. Subscripts are the possible spin contributions from the occupied valence orbitals forming the configurations at the oblate ($\gamma = 60°$) axis. Similarly, for $(\pi, \alpha) = (-, 0), (-, 1)$, the configurations and the possible maximum spins are [03,14], *i.e.*

[a] e-mail: dongbg@iris.ciae.ac.cn

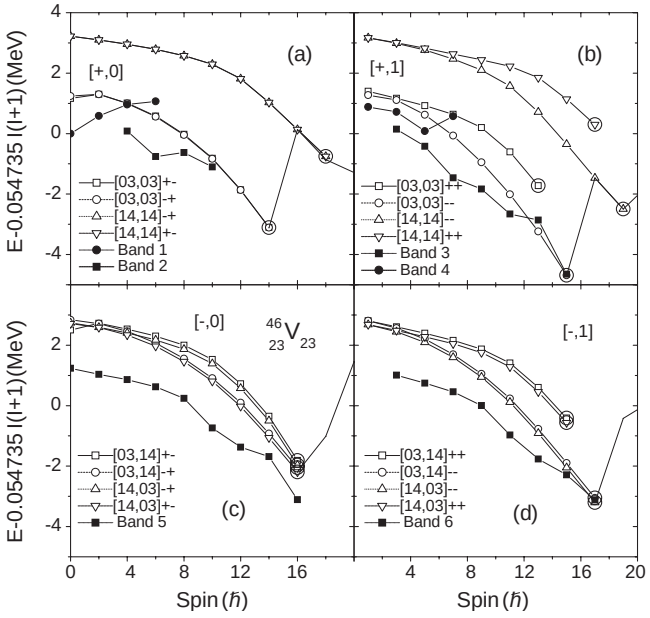


**Fig. 1.** Energies plotted as a function of spin for the calculated and observed bands in $^{46}$V. The energies are given relative to a rigid rotation reference $(\hbar^2/2J_{\rm rig})I(I+1)$. The calculated yrast lines are indicated by dotted lines. The open symbols indicate the theoretical data and solid symbols the experimental data. Terminating states are indicated by large open circles.

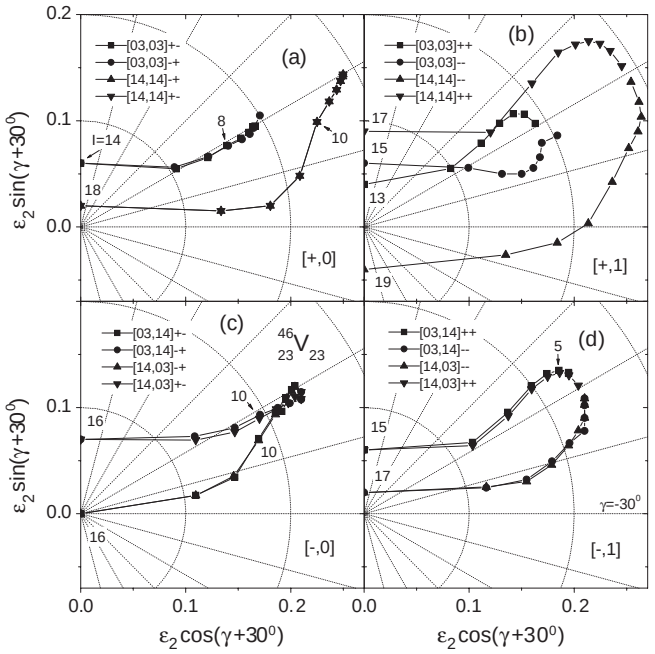


**Fig. 2.** Calculated shape trajectories as a function of spin in the $(\varepsilon_2,\gamma)$-plane for calculated bands in $^{46}$V corresponding to fig. 1. The step in spin in the curves is $2\hbar$.

$\pi[(f_{7/2})^{3\pm}_{6.5,7.5}]_{6.5,7.5} \otimes \nu[(d_{3/2}s_{1/2})^{-1\pm}_{0.5,1.5}(f_{7/2})^4_8]_{8.5,9.5}$, and $I_{\rm max} = 15, 16$ and 17, and [14,03], $\pi[(d_{3/2}s_{1/2})^{-1\pm}_{0.5,1.5}(f_{7/2})^4_8]_{8.5,9.5} \otimes \nu[(f_{7/2})^{3\pm}_{6.5,7.5}]_{6.5,7.5}$, and $I_{\rm max} = 15, 16$ and 17, respectively.

The experimental and theoretical $E - E_{\rm RLD}$ curves as a function of spin for near yrast bands for the four combinations of parity $\pi$ and signature $\alpha$ are shown in fig. 1. Based on the calculated results, for $^{46}$V, the configurations [03,03]+− (or [03,03]−+), [03,03]−−, [14,03]+− and [14,03]−− with parity and signature $(\pi,\alpha) = (+,0)$, $(+,1)$, $(-,0)$ and $(-,1)$ are assigned to the observed bands 2, 3, 5 and 6, respectively. Comparing the results shown in figs. 1 and 2, it can be seen that the three observed bands 3, 5 and 6 have been observed up to their terminating states having the terminating spins of 15, 16 and 17, respectively, and the calculated bands are in good agreement with the observed bands both in the relative energies and in the curvature at high spin without normalization, especially for terminating states, which are in the spin region of interest. In the low-spin range, the calculated bands are approximately 1 MeV above the corresponding observed bands because the CNS model used here has neglected pairing interactions which would play an important role at low spin. The good agreement between calculated and observed bands at high spin without normalization confirms that the CNS approach works very well in the $A \sim 40$ mass region.

There is no shape coexistence within the same configuration on the potential-energy surfaces for all configurations near yrast lines in $^{46}$V for the whole spin region but there would be shape coexistence among the different configurations. The process of smooth band termination and the change in the intrinsic nuclear shape of the interesting bands as a function of spin in $^{46}$V are shown in fig. 2 by the calculated shape trajectories in the $(\varepsilon_2,\gamma)$-deformation plane. All observed bands are normal-deformed bands according to the calculations. The $\gamma$-deformations of the specific configurations are always positive or very close to zero when the proton or neutron $(d_{3/2}s_{1/2})^{-1+}(f_{7/2})^4$ configuration is included. This is because the orbital [330]1/2 belonging to the $f_{7/2}$ subshell with $\alpha = -1/2$ and [202]3/2 with $\alpha = +1/2$ when $\gamma$ is positive is much lower in energy than that when $\gamma$ is negative at $\varepsilon_2 = 0.18$, see fig. 3(a). The [330]1/2 orbital with $\alpha = -1/2$ is always occupied at normal deformations in all configurations considered here and the rest of the valence orbitals [330]1/2, [321]3/2 and [202]3/2 have relative weak effect on decreasing energy when $\gamma$ is negative. For some configurations, *e.g.* [03,03] with $\alpha = 0$, the increasing and decreasing effect on the energy is almost or just balanced so the deformation is very close to or on the prolate ($\gamma = 0°$) axis at a deformation $\varepsilon_2 = 0.1 \sim 0.2$. The decreasing effect of the [321]3/2 orbital with $\alpha = -1/2$ for negative $\gamma$ on the energy is stronger than that with $\alpha = +1/2$ so the $\gamma$-deformation of the configuration [03,03]−− is negative and [03,03]++ positive. The last valence proton and neutron in the same [321]3/2 orbital with the same signature make such decreasing effect of different signature on energy stronger. The [14,14]−− configuration with both proton and neutron [202]3/2 orbital with $\alpha = +1/2$ unoccupied has the largest negative $\gamma$-deformation since this orbital has the strongest decreasing effect for positive $\gamma$ among these configurations, see fig. 2. Figure 3(b) shows the effect of the $\gamma$-deformation on the total energy for $^{38}$K. We have formed

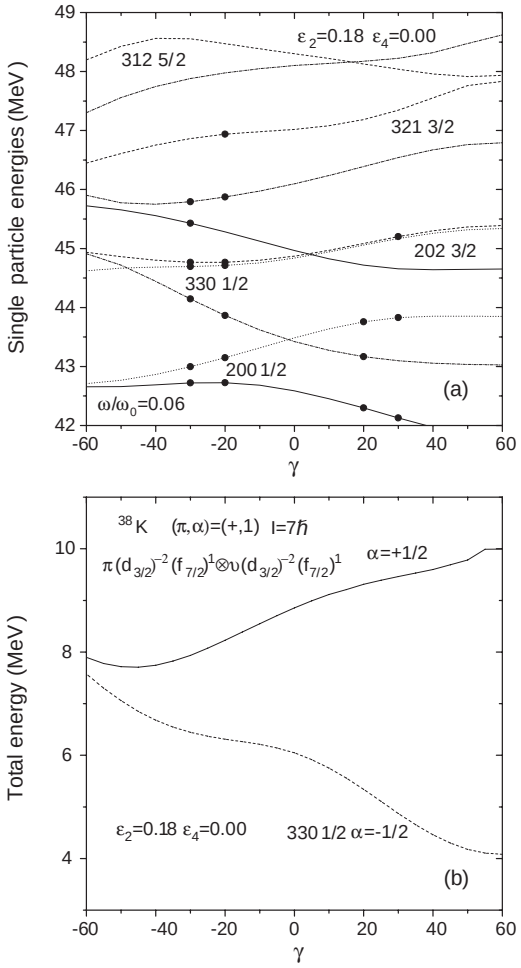


**Fig. 3.** (a) Single-proton energies plotted as a function of the $\gamma$-deformation. The solid, dotted, dashed and dot-dashed lines are for parity and signature (+,0), (+,1), (−,0) and (−,1), respectively. The solid circles indicate the orbitals occupied by the proton configurations 03 and 14 for $^{46}$V and 21 with the $f_{7/2}$ proton in the [330]1/2 orbital with $\alpha = -1/2$ and +1/2 for $^{38}$K. (b) Total energies as a function of the deformation $\gamma$ for $^{38}$K. The solid (dashed) line indicates the total energies of the configuration with the $f_{7/2}$ proton and neutron in the $\alpha = +1/2$ $(-1/2)$ orbital.

the configurations for $^{38}$K by making both the last proton and neutron occupy the [330]1/2 orbital with the same signature $\alpha = -1/2$ or +1/2 so that it makes the effect of the $\gamma$-deformation double. For a special number of nucleons, such as one nucleon outside a core of fulfilled closed shell or nucleus at special deformation, the CNS approach could firmly distinguish the difference of configurations to only one orbital in the rotating frame but it could not in general [11]. The configurations [01,01]++ and [01,01]−−, $\pi(f_{7/2})^{1\pm} \otimes \nu(f_{7/2})^{1\pm}$, for $^{38}$K at special deformations $\varepsilon_2 = 0.18$ and $\varepsilon_4 = 0.00$ formed by the [330]1/2 orbital with different signature $\alpha = -1/2$ or +1/2 and the rest orbitals occupied are the same, are an example to show such effect, see fig. 3.

Two configurations [03,03]+− and [03,03]−+ or [14,14]+− and [14,14]−+ in fig. 1(a) are degenerate. There are almost degenerate configurations with $\alpha = 0$ or 1 and negative parity. The two degenerate configurations [03,03] or [14,14] are formed by exchanging proton and neutron configuration only. Here we keep the two configurations because the CNS model does not include isospin interaction and the real configuration should be the combination of the different isospin states. The qualitative explanation of the effect of proton-neutron ($pn$) pairing on the energy is that the effect is dominated by the energy difference between the proton and neutron Fermi surfaces. If the energy difference is small, the effect would play an important role, but if the difference is large, that effect could be neglected. In the CNS calculations, there are two kinds of Fermi surfaces from the discrete and smoothed single-particle energy sums for proton, neutron and each rotational frequency value. For example, the energy difference of the proton and neutron Fermi surfaces at $(\varepsilon_2, \gamma) = (0.14, -9^\circ)$ at $\omega = 0.05\omega_0$ for the [03,03]−− configuration with $(\pi, \alpha) = (+, 1)$ is about 0.14 MeV for both discrete (4.121 and 4.133 $\hbar\omega_0$) and smoothed (4.048 and 4.061 $\hbar\omega_0$) sums. The good agreement between calculated and observed bands at high spin without normalization indicates that pairing, including $pn$ pairing, could be neglected in the high-spin region for odd-odd nucleus $^{46}$V but it could play an important role in the low-spin region, see fig. 1. We will not discuss this further in the CNS model.

For $^{50}$Mn, the calculated and observed bands as a function of spin are shown in fig. 4(a). Since there is only one observed high-spin band, here only the calculated bands with the same parity and signature $(\pi, \alpha) = (+, 1)$ as the observed one are shown. The possible terminating states are built at maximum spin in the [05,05] configurations: $\pi[(f_{7/2})^{5\pm}_{6.5,7.5}]_{6.5,7.5} \otimes \nu[(f_{7/2})^{5\pm}_{6.5,7.5}]_{6.5,7.5} = 13, 14$ (for $\alpha = 0$) and 15, respectively. The [05,05]−− configuration is assigned to the observed band 1. Comparing with the CNS calculated results, the observed band 1 has been observed up to its terminating state having the terminating spin of 15, and it is a normal-deformed band, see fig. 4(b). Similar to the band structures in $^{46}$V, the calculated configurations [05,05]−+ and [05,05]+− with parity and signature $(\pi, \alpha) = (+, 0)$ are degenerate and yrast, [16,05]−+ and [16,05]−− are yrast for $(-, 0)$ and $(-, 1)$, reached their terminating states at spin 14, 14, 14 and 15, respectively.

Comparing the rotational behavior of the calculated rotational bands in $^{46}$V and $^{50}$Mn with rotation around the axis with the middle moment of inertia, which is forbidden in classical mechanics rotation, described in ref. [9] in $^{48}$Cr, conclusions of the rotation around the intermediate axis can be drawn for $^{46}$V and $^{50}$Mn. The calculated configurations that clearly show rotation around the intermediate axis are [03,03]−− with $(\pi, \alpha) = (+, 1)$, and [14,03]−− with $(-, 1)$ in $^{46}$V so the observed bands 3 and 6 would be bands with rotation around the intermediate axis. Similarly, the calculated configuration [05,05]−− and observed band 1 in $^{50}$Mn clearly show rotation around the intermediate axis. All these bands with rotation around the intermediate axis should be confirmed further by

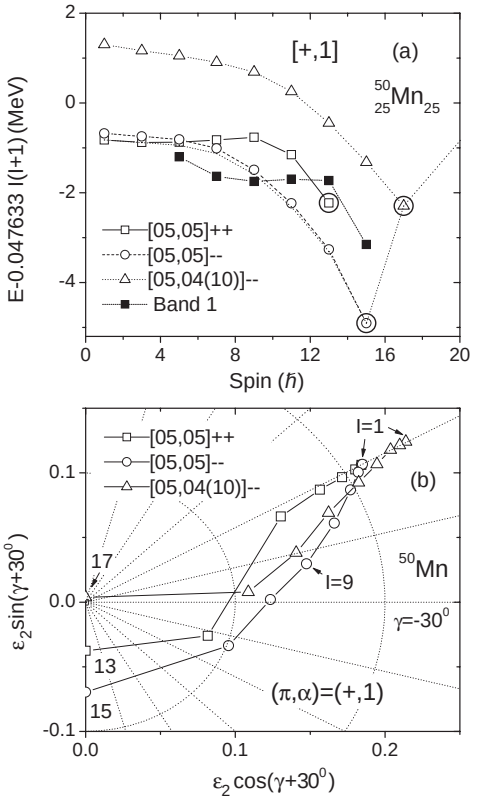


**Fig. 4.** (a) Energies plotted as a function of spin for the calculated and observed bands in $^{50}$Mn for parity and signature $(\pi, \alpha) = (+, 1)$. Terminating states are indicated by large open circles. (b) Calculated shape trajectories as a function of spin in the $(\varepsilon_2, \gamma)$-plane for calculated bands in the top panel in $^{50}$Mn. (10) means one neutron in the $f_{5/2}p_{3/2}p_{1/2}$ orbitals.

calculating $B(E2)$ values and spectroscopic quadruple moments as that of ref. [9] and we will not discuss them here.

In summary, band structures near yrast lines of the $Z = N$ odd-odd nuclei $^{46}$V and $^{50}$Mn in the $A \sim 40$ mass region have been investigated and the calculated bands show good agreement with observed bands at high spin. The terminating states in $^{46}$V and $^{50}$Mn have been confirmed by the calculations. Both nuclei are normal deformed and with no shape coexistence within the same configuration. All these show the CNS model works well in the $A \sim 40$ mass region. Possible bands with rotation around the intermediate axis and the effect of $\gamma$-deformation on the total energy of several interesting configurations are discussed.

We would like to thank I. Ragnarsson for access to the CNS code. This work has been partially supported by the Theoretical Nuclear Physics Foundation of the Department of Nuclear Physics, China Institute of Atomic Energy, and the Foundation of the Center of Theoretical Nuclear Physics, National Laboratory of Heavy Ion Accelerator of Lanzhou.

## References

1. F. Brandolini *et al.*, Phys. Rev. C **64**, 044307 (2001).
2. C. Friebner *et al.*, Phys. Rev. C **60**, 011304 (1999).
3. S.M. Lenzi *et al.*, Phys. Rev. C **60**, 021303 (1999).
4. C.E. Svensson *et al.*, Phys. Rev. C **58**, R2621 (1998).
5. A. Schmidt *et al.*, Phys. Rev. C **62**, 044319 (2000).
6. T. Bengtsson, I. Ragnarsson, Nucl. Phys. A **436**, 14 (1985).
7. A.V. Afanasjev, I. Ragnarsson, Nucl. Phys. A **591**, 387 (1995).
8. J.-y. Zhang *et al.*, Phys. Rev. C **39**, 714 (1989).
9. A. Juodagalvis *et al.*,Phys. Lett. B **477**, 66 (2000).
10. C.E. Svensson *et al.*, Phys. Rev. Lett. **85**, 2693 (2000).
11. A.V. Afanasjev *et al.*, Phys. Rep. **322**, 1 (1999).